

Petrology and geochemistry of Aligoodarz granitoid, Western Iran: implications for petrogenetic relation with Boroujerd and Dehno granitoids

Amir Esna-Ashari^{1*}, Mohammad-Vali Valizadeh¹, Abolfazl Soltani², Ali-Asghar Sepahi³

¹ School of Geology, College of Science, University of Tehran, Tehran, Iran

² School of Civil Eng., University of Shahid Rajaei, Lavizan, 1678815811, Tehran, Iran

³ Department of Geology, Faculty of Science, Bu-Ali Sina University, Hamadan, Iran

*Corresponding author, e-mail: aashari@ut.ac.ir

(received: 22/11/2010 ; accepted: 19/10/2011)

Abstract

The Aligoodarz granitoid occurs in Sanandaj-Sirjan Zone (SSZ), Western Iran. Tonalite, granodiorite and granite are the main rock types cropping out in the area. Comparison of Aligoodarz granitoid with Dehno and Boroujerd granitoids reveals several similarities in their chemical characteristics. Thus, the above mentioned granitoids can be assigned as a co-genetic magmatic suite, in which plutons evolved from a parental magma; with fractional crystallization being the main mechanism for magma evolution. Samples with lower SiO₂ content from different areas, are not similar in composition, and indicating varying degrees of mineral accumulation and trapped interstitial melts. These granitoids are compositionally similar to normal I-type granitoid rocks originated from continental arcs. Compared with the primordial mantle, they are enriched in Large Ion Lithophile Elements (LILE) and Light Rare Earth Elements (LREE) over High Field Strength Elements (HFSE) and Heavy Rare Earth Elements (HREE). This feature together with relative depletion of Ta, Nb, Ti, and P confirm derivation of these granitoids from a crustal source region in continental arc environment.

Key words: Sanandaj-Sirjan, Iran, Granitoid, Geochemistry, Arc-type magmatism

Introduction

From the Late Precambrian to Permian times, Persian platform was composed of several microcontinents and it was part of the Afro-Arabian (Gondwana) continent (Golonka, 2000; Heydari, 2008). During the Early Permian, some of these microcontinents collectively referred to as the Cimmerian continent separated from the Gondwana land, formed the Neo-Tethys Ocean (Fig. 1a) (Dercourt *et al.*, 1986; Kazmin, 1991; Stampfli *et al.*, 1991; Golonka, 2000; Heydari, 2008).

Central Iran Plate (CIP) which had been part of the Cimmerian continent, connected to the Eurasia as the result of closure of Paleo-Tethys in Middle-Late Triassic. Then during Triassic to Jurassic times, Arabian plate separated from the Gondwana and its subsequent movement to the Eurasia initiated. This resulted in the subduction of Neo-Tethys oceanic crust underneath the CIP (Berberian & King, 1981; Berberian &

Berberian, 1981; Hooper *et al.*, 1994). This subduction progressively closed the Neo-Tethys ocean and formed the Zagros Orogenic Belt of Iran (Berberian and King, 1981; Alavi, 1980, 1994; Golonka, 2000). The subduction of Tethyan oceanic crust yielded to the collision of Arabian-CIP that might have taken place during the Late Cretaceous–Early Tertiary (Berberian & Berberian, 1981; Berberian & King, 1981; Alavi, 1994; Mohajjel and Fergussen, 2000; Alavi, 2004).

The Zagros Orogenic Belt of Iran (Fig. 1b) is part of the Alpine-Himalayan orogenic system and consists of three parallel tectonic subdivisions (Alavi, 2004) from northwest to southeast, including the Urumieh-Dokhtar Volcanic Belt (UDVB), the Sanandaj-Sirjan Zone (SSZ) and the Zagros Fold-Thrust Belt (ZFTB).

During most of the second half of the Mesozoic, the SSZ represented an active

continental arc margin whose calc-alkaline magmatic activity progressively shifted northward (Berberian & King, 1981; Sengör, 1990) and resulted in the intrusion of many granitoid plutons with different origin. For example the Alvand pluton is reported as S-type (Sepahi, 2008) while Boroujerd (Ahmadi Khalaji *et al.*, 2007) and Siah-Kuh (Arvin *et al.*, 2007) are I-type in nature. A-type granites are also reported in some areas of the SSZ (Shabanian *et al.*, 2008; Sepahi & Athari,

2006).

The present work investigates petrographic and whole-rock geochemical characteristics of Aligoodarz granitoid rocks that occur in the central part of the SSZ (Figs. 1c-d). By comparing the chemical features of Aligoodarz granitoid rocks with those from Dehno (Rajaieh, 2005) and Boroujerd (Ahmadi Khalaji *et al.*, 2007) granitoids (Fig. 1c) some light can be shed on the origin and tectonic setting of the Aligoodarzpluton..

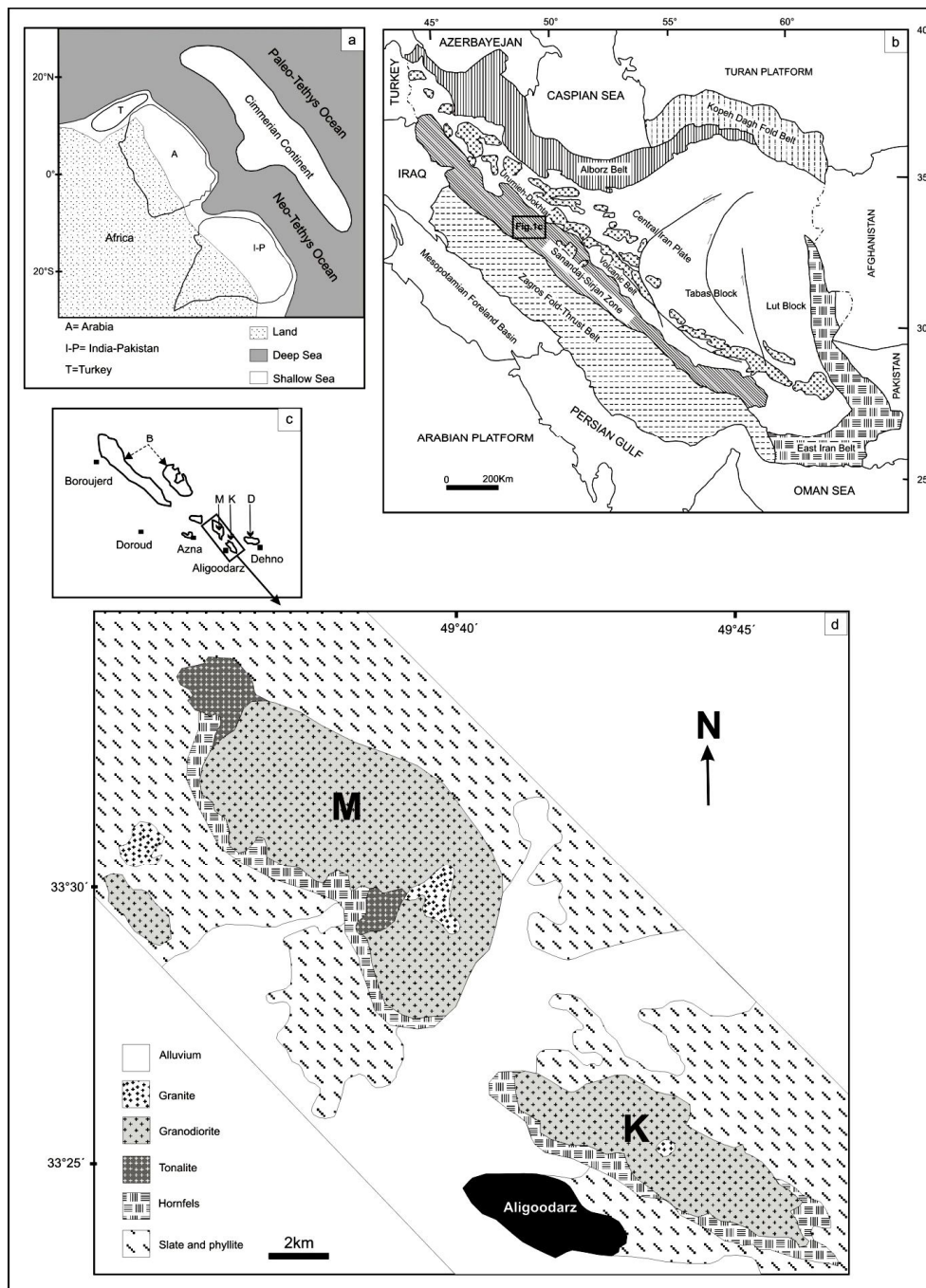


Figure 1: a) Separation of Cimmerian continent from the Persian platform during the opening of the Neo-Tethys Ocean in Early Permian (after Heydari, 2008); b) Generalized tectonic map of Iran, based on geological maps of Ruttner & Stocklin (1967) and Alavi (1991); c) Distribution of major igneous bodies in an area shown by a rectangle in the Sanandaj-Sirjan Zone. (B = Boroujerd; M = Mollataleb; K = Khorheh; D = Dehno); d) Simplified geological map of the Aligoodarz granitoid. M and K are the two main granitoid outcrops in this area.

Geological Setting

The SSZ, located southwest of the Urumieh-Dokhtar Volcanic Belt, is characterized by metamorphic and complexly deformed rocks which are in turn intruded by deformed and undeformed plutons and associated Mesozoic

volcanic rocks. SSZ is 1500 km long and up to 200km wide and extends in a northwest (Sanandaj) to southeast (Sirjan) direction (Fig.1b). The rocks of this zone are mostly Mesozoic in age (Valizadeh & Cantagrel, 1975; Masoudi, 1997; Ahmadi Khalaji, *et al.*, 2007).

Paleozoic rocks are rarely exposed in the northwestern part of the SSZ, but they commonly occur in the southeastern part (Berberian, 1995; Sabzehei & Eshraghi, 1995; Hassanzadeh *et al.*, 2008). The major deformation and metamorphic events that affected the SSZ are associated with the opening and closure of the Neo-Tethys ocean during the Mesozoic (e.g. Alavi, 1994).

The Aligoodarz granitoid located in 300 km southwest of Tehran between the 33°23'-34°N and 49°32'-55°E (Fig. 1). The Khorheh and Mollataleb are two main outcrops of the granitoid rocks in this area. The latter is known as Azna granitoid by Moazzen, *et al.*, (2004). They are elongated in NW-SE trending and their long axes are parallel or sub-parallel to the main trend of SSZ. The Aligoodarz granitoid is surrounded by low-grade metamorphic aureole and intruded into the late Triassic to Jurassic regional metamorphic slates and phyllites called Hamadan phyllite (Mohajjel, *et al.*, 2003).

Field relation

The Aligoodarz granitoid crops out in two localities namely Mollataleb (M) and Khorheh (K) (Figure 1d). According to the field evidence and detailed mapping of the area, the Aligoodarz granitoid occurs as three main different rock types including tonalite, granodiorite and granite. Contacts between these lithologies are sharp. Granite occurs as fine-grained leucocratic dikes (Fig. 2b) and small stocks intruding the granodiorite. Along the contact of granodiorite and tonalite a kind of coarse-grained enclaves occur in the granodiorite (Fig. 2a). These enclaves which are closely spaced and seem to be fragments of the tonalite caught in the intruding granodiorite, are coarse grained and petrographically similar to the adjacent tonalite. They exhibit angular forms which indicate their disrupted nature and closeness to the source region.

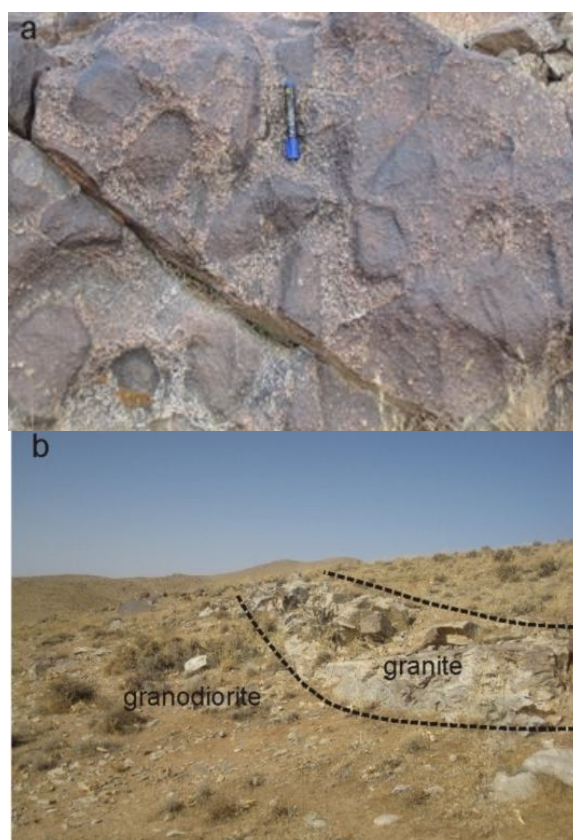


Figure 2: (a) Disrupted fragments of tonalite enclosed in granodiorite observed in the boundary of tonalite and granodiorite; (b) intrusion of granites as felsic dykes into the granodiorite.

Petrography

Tonalite

Tonalite is fine to medium-grained in texture and has less contents of quartz and K-feldspar/plagioclase ratio compared with granodiorite and granite (Figs. 3a-b) but it has higher modal content of total ferromagnesian minerals. Its major mineral contents include amphibole, biotite, quartz and plagioclase (table 1). Minor mineral components are zircon, apatite, magnetite, rutile and Fe-Ti oxides. Plagioclase is occasionally altered to sericite. Chlorite occurs as secondary mineral after amphibole and/or biotite alteration. Amphibole grains occur either as prismatic crystals or as anhedral grains. Plagioclase occurs as zoned euhedral to subhedral crystals with oscillatory zoning revealed by EMP analyses (not presented here).

Granodiorite

The granodiorite, the main rock type occurring in the area, is medium to coarse-grained. Plagioclase, quartz, biotite and K-feldspar are the major mineral components of the granodiorite (table 1 and Figs. 3c-d). Plagioclase is occasionally altered to sericite. Plagioclase crystals display oscillatory zoning indicating disequilibrium system. K-feldspars include orthoclase and microcline. Accessory minerals are zircon, magnetite, tourmaline, rutile and apatite. Slight alteration to muscovite and/or titanite and Fe-Ti oxides are commonly observed in biotite crystals. Biotite is highly pleochroic and contain apatite and zircon inclusions.

Mollataleb and Khorheh granodiorites are similar in mineralogy and whole-rock chemistry but different in textural features. Mollataleb granodiorite is variably strained and displays a clear foliation as evidenced from minerals orientation, particularly biotite. Quartz represents anhedral crystals, strongly recrystallised and displays undulatory extinction which is typical of solid-state deformation (Fig. 3c). There is no evidence of deformation in Khorheh granodiorite, it displays poikilitic texture, with inclusions of biotite and plagioclase occurring in large optically continuous crystals of K-feldspar and quartz (Fig. 3d).

Granite

Granite as the late stage intrusion is essentially fine-grained. Its main mineral assemblages include: quartz, K-feldspars and plagioclase (table 1) by volume. Muscovite, biotite, tourmaline, zircon and apatite occurs as accessory minerals. Muscovite seems to be mostly secondary mineral after feldspar alteration. The granite is light in color with a

hypidiomorphic granular texture (Fig. 3e).

Analytical Techniques

Out of 150 samples collected from different localities described above, 90 samples were selected for microscopic studies and 21 samples for whole rock geochemical analyses. Rock specimens of 2–3 kg in weight were crushed and powdered. Major and trace element concentrations were determined respectively by Inductively Coupled Plasma-Atomic Emission Spectrometry (ICP-AES) and Inductively Coupled Plasma-Mass Spectrometry (ICP-MS) at ALS Chemex laboratories in Vancouver, Canada. The precision is better than $\pm 2\%$ for major elements and $\pm 5\%$ for trace elements. Details of the analytical processes are accessible at www.alschemex.com.

Geochemistry

Analyses of 21 samples, mostly from the granodiorite, are listed in Table 2. Mollataleb samples correspond to highly deformed rocks but no systematic compositional differences were observed in these rocks, compared with those of Khorheh. It means that all major- and trace-element compositions are not affected by late stage deformation and can be considered as primary. To compare the Aligoodarz granitoid with those of in Dehno (Rajaieh, 2005) and Boroujerd (Ahmadi Khalaji *et al.*, 2007), the whole rock geochemical data base of the latter are included in the present work. Tonalite, granodiorite and granite are the major rock types in Boroujerd but Dehno area is predominant by granodiorite. To eliminate any ambiguity, it is desirable to consider the studied granitoids into two categories including intermediate for tonalitic rocks and felsic for granodioritic and granitic rocks.

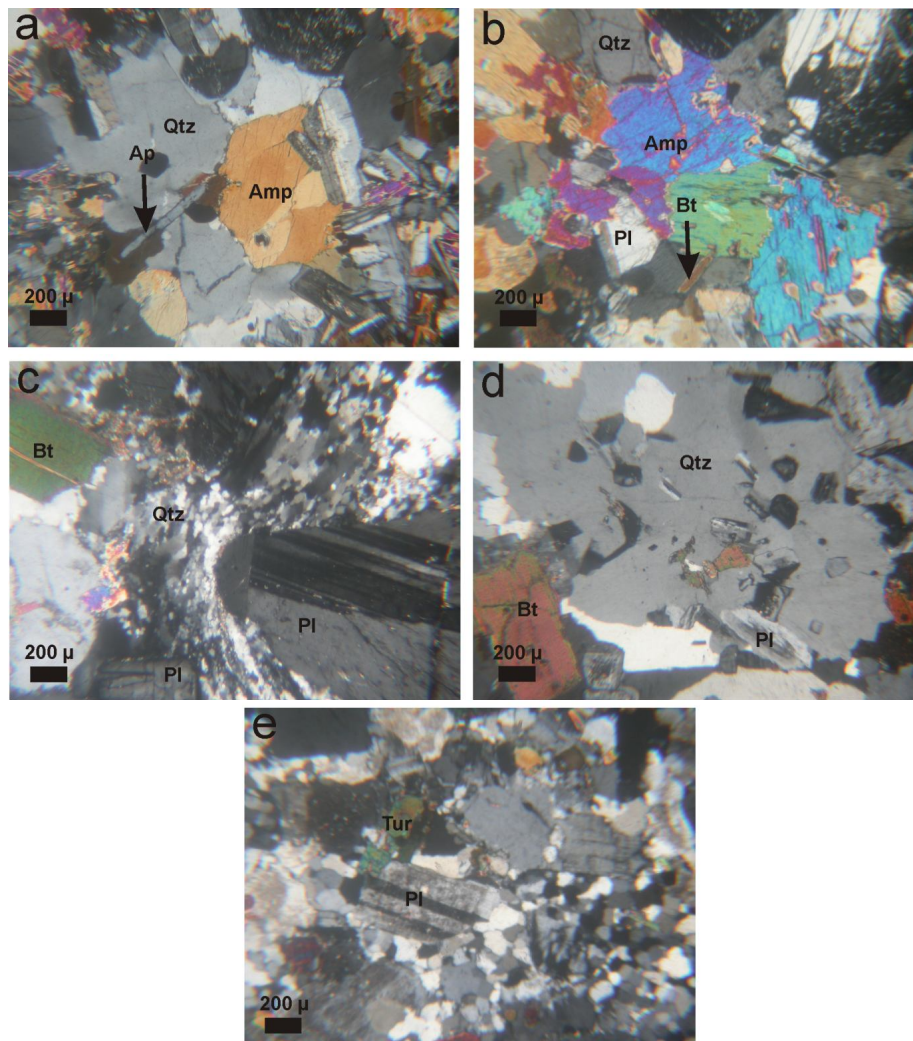


Figure 3: Photomicrographs of tonalite (a and b), granodiorites (c and d) and granite (e) of the Aligoodarz area (taken in XPL state). Tonalite is characterized by abundant amphibole. The Khorheh granodiorite (d) shows poikilitic texture with no evidence of quartz recrystallization, Granodiorite of the Mollataleb (c) is highly deformed. (abbreviations include : Amp = Amphibole; Ap = Apatite; Bt = Biotite; Pl = Plagioclase; Qtz = Quartz; Tur = Tourmaline).

Table 1: representative modal analyses of the Aligoodarz granitoids

Rock type	sample	Pl	Bt	Qtz	Kfs	Amph
Tonalite	AL11	45.9	13.0	16.0	1.4	23.7
	AL75	31.9	24.5	17.3	1.5	24.9
	AL88	41.3	8.2	16.1	1.8	32.6
	AL90	24.6	4.2	6.6	1.5	63.2
Granodiorite	B07	42.3	17.0	30.0	10.7	0.0
	AL27	26.4	19.3	50.6	3.6	0.0
	AL19	36.0	22.5	37.0	4.4	0.0
	B05	38.0	17.7	33.1	11.2	0.0
	AL44	34.4	18.0	37.0	10.7	0.0
	AL55	35.7	18.6	31.5	14.3	0.0
Granite	AL21-2	10.4	<1	47.5	42.1	0.0
	AL20	9.1	2.4	58.3	30.1	0.0

Major elements

The content of SiO₂ in Aligoodarz granitoid

varies from 52 to 75 wt%. Similarly, wide range in the contents of Al_2O_3 , Fe_2O_3 , MgO and CaO is observed. Samples from Aligoodarz have relatively high content of total Fe as Fe_2O_3 . They have up to 9 wt% Fe_2O_3 contents in tonalite and more than 5 wt% in granodiorite samples but extend in more light colored variants (granites) to about 1wt% Fe_2O_3 contents.

Using SiO_2 as a fractionation index, samples display chemical variations and clear trends on Harker diagrams (Fig. 4). Most of the plotted samples display meaningful trends on variation diagrams. In all diagrams, Dehno granodiorites plot close to the Aligoodarz granodiorites but they are relatively scattered probably due to variable degree of alteration. With increasing SiO_2 , the contents of TiO_2 , Fe_2O_3 , CaO, Al_2O_3 and MgO decrease but K_2O and Na_2O increase. The plot of K_2O versus SiO_2 (Fig. 4) indicates that the Aligoodarz granitoid is calc-alkaline with medium to high content of potassium. On Fe_2O_3 and CaO diagrams, samples show the least degree of scattering (Fig. 4). Plots of Al_2O_3 , MgO and TiO_2 decrease with increasing SiO_2 . They show a convergence of points into a tight array at high SiO_2 values but diverge markedly at the low SiO_2 end. Relative to Boroujerd granitoid, those in Aligoodarz and Dehno have higher abundance of Na_2O and K_2O .

The Aligoodarz granitoid is metaluminous to peraluminous with ASI values ranging from 0.63 to 1.23. These values are based on $\text{Al}_2\text{O}_3 / (\text{CaO} + \text{Na}_2\text{O} + \text{K}_2\text{O})$ molar ratio of Shand (1943) which is the most useful chemical discriminant between metaluminous (ASI <1) and peraluminous (ASI >1) granitoids (Fig. 5). Since a degree of Al-oversaturation is an intrinsic property of most felsic granite melts, the ASI value increases with increasing SiO_2 . Tonalite samples with the lowest SiO_2 content are metaluminous with average ASI value of 0.9 but granodiorites and granites with higher SiO_2 contents are slightly peraluminous with average ASI values of 1.14 and 1.20, respectively.

Trace elements

On the trace elements vs. SiO_2 variation diagrams that are presented in Figure 6, Co, V, Cr, and Ni decrease but Rb increases with increasing SiO_2 . The content of Sr versus SiO_2 shows slightly scattering with a general trend of decreasing towards more felsic variants. It is noticeable that the Aligoodarz tonalites have lower Sr content relative to the rocks of Boroujerd. However, two samples of Boroujerd, which are characterized by the lowest content of SiO_2 , plot close to the Aligoodarz tonalites.

In Figure 7 the elemental ratios have been plotted against SiO_2 contents. The variation trend of Sr/Ba for the samples having less than ~68 wt% SiO_2 is negative. This ratio slightly increases as the SiO_2 content exceeds ~68 wt%. Nb/Ta ratio shows a decreasing trend and the noticeable point is that the intermediate (tonalite) and felsic (granodiorite + granite) rocks do not represent a compositional continuum.

The Rare Earth Elements (REE) concentrations of Aligoodarz granitoid were normalized to chondrite values of Boynton (1984) (Figure 8). The REE patterns for intermediate (tonalite) and felsic (granite and granodiorite) rocks are relatively similar. The $(\text{La}/\text{Lu})_N$ ratios for granodiorite, tonalite and granite are 9.38, 5.27 and 3.63 respectively, indicating a moderate Light Rare Earth Elements (LREE) enrichment. The Eu anomalies show an average of 0.87 for tonalite, 0.54 for granodiorite and 0.41 for granite (table 2). The $\sum\text{REE}$, respectively for granite, tonalite and granodiorite is 8-13, 12-15 and 31-40 times chondrite-normalized values and there is a general increase in the total REE from tonalite to granodiorite but this trend is reversed for granites. Figure 9 shows the chondrite-normalized REE patterns for average REE in the Aligoodarz, Dehno and Boroujerd granodiorites and it is noticeable that the REE patterns of all the granodiorites are very similar.

Table 2: Major and trace element contents of the Aligoodarz granitoid.

Sample	tonalite				granodiorite												granite					
	AL75	AL88	AL90	AL11	AL60	AL36	B05	AL41	AL44	AL55	B07	AL12	AL14	AL19	AL25	AL27	AL28	AL20	AL21-2	AL58	AL72	
wt%																						
SiO ₂	55.2	53.2	52.6	54.4	66.5	65.4	67.9	66.3	66.3	64.6	66.0	65.9	67.7	65.6	66.0	66.0	68.3	75.6	73.5	73.5	75.2	
Al ₂ O ₃	15.3	18.3	12.4	17.1	15.0	15.6	14.9	15.6	15.6	16.0	15.8	15.4	14.8	15.8	15.6	15.1	14.3	13.7	13.9	14.6	13.9	
Fe ₂ O ₃	9.3	9.8	8.9	7.9	4.9	5.4	5.4	5.6	5.3	5.9	5.1	5.7	5.0	5.1	5.1	5.0	3.9	1.0	1.0	1.5	1.1	
CaO	6.3	8.5	9.5	8.0	2.7	3.4	3.2	3.2	3.2	3.4	3.3	3.6	3.2	3.6	3.2	3.2	2.3	0.7	0.6	1.1	0.6	
MgO	8.1	5.8	12.7	7.5	1.4	1.4	1.4	1.7	1.4	1.7	1.5	1.8	1.5	1.6	1.6	1.6	1.0	0.2	0.1	0.2	0.2	
Na ₂ O	0.9	1.3	1.1	1.0	2.4	2.5	2.4	2.4	2.5	2.5	2.7	2.5	2.6	2.6	2.5	2.3	2.4	3.0	3.0	3.1	3.4	
K ₂ O	1.5	1.0	0.6	0.7	3.5	3.1	3.4	3.2	3.3	3.4	3.3	3.1	3.0	2.7	3.2	3.1	4.2	4.7	5.2	4.5	4.3	
TiO ₂	0.61	0.58	0.53	0.37	0.52	0.58	0.64	0.64	0.55	0.59	0.63	0.72	0.65	0.59	0.60	0.60	0.46	0.05	0.03	0.06	0.05	
MnO	0.18	0.19	0.18	0.14	0.10	0.11	0.10	0.11	0.11	0.10	0.10	0.11	0.09	0.10	0.10	0.09	0.07	0.06	0.02	0.03	0.03	
P ₂ O ₅	0.08	0.18	0.08	nd	0.15	0.15	0.14	0.15	0.15	0.14	0.12	0.13	0.14	0.14	0.17	0.20	0.13	0.13	0.17	0.18	0.20	
LOI	2.42	1.36	1.55	1.56	1.47	1.48	1.08	0.49	1.28	1.64	1.28	0.98	1.44	0.88	0.70	1.09	0.96	0.79	0.79	1.17	0.89	
total	99.9	100.2	99.9	98.7	98.6	99.0	100.6	99.3	99.6	99.8	99.8	99.9	100.2	98.7	98.6	98.3	97.9	99.9	98.3	100.0	99.8	
ppm																						
Ba	184	121	69	111	356	329	389	347	345	399	359	350	398	291	332	393	401	103	67	406	67	
Ce	26.1	27.6	18.6	25.4	75.8	71.8	72.7	73.0	63.0	56.5	70.2	74.5	76.6	76.9	72.5	81.5	59.4	20.4	14.2	27.0	13.7	
Co	34.0	31.3	43.7	34.4	9.9	10.1	10.3	12.9	10.4	12.0	11.5	12.8	10.1	11.8	11.3	12.0	8.1	1.2	1.8	1.8	1.0	
Cr	690	170	1240	580	50	40	40	60	40	60	50	70	50	60	60	30	30	10	10	10	10	
Cs	4.9	8.7	2.0	2.8	8.0	7.3	6.6	8.5	9.0	7.1	9.3	7.6	6.7	7.9	16.4	8.4	6.3	4.4	4.9	4.9	6.2	
Dy	2.5	2.4	2.7	2.2	4.8	4.5	4.7	5.3	5.0	3.8	5.4	5.0	5.0	4.8	4.8	5.6	5.4	3.0	1.8	1.3	1.8	
Er	1.6	1.5	1.6	1.5	2.6	2.6	2.9	3.1	2.9	2.2	3.2	3.1	2.9	2.6	2.6	3.2	3.4	2.0	1.1	0.5	1.1	
Eu	0.7	0.8	0.6	0.7	1.0	1.1	1.0	1.1	1.0	1.0	1.1	1.1	1.1	1.2	1.1	1.2	1.0	0.3	0.2	0.8	0.1	
Ga	16.8	19.4	12.4	17.3	19.5	20.0	19.3	19.7	19.8	20.3	21.1	20.6	20.1	19.9	19.9	21.2	16.8	13.4	15.0	20.2	16.9	
Gd	2.5	2.6	2.3	2.4	6.4	5.9	5.8	6.4	5.6	4.6	6.2	6.3	6.4	6.5	6.2	7.0	5.6	2.1	1.5	2.7	1.3	
Hf	1.5	1.7	2.2	1.4	5.8	5.3	4.8	5.7	5.0	5.6	5.1	5.7	5.3	5.4	5.3	5.3	4.3	1.9	1.6	2.5	1.5	
Ho	0.5	0.5	0.6	0.5	0.9	0.9	0.9	1.1	1.0	0.7	1.1	1.0	1.0	0.9	0.9	1.1	1.1	0.7	0.4	0.2	0.4	
La	13.3	13.7	8.6	11.8	37.8	35.9	34.9	36.1	30.9	27.9	33.3	35.6	37.1	37.8	35.5	40.2	29.3	10.3	7.4	12.9	7.3	
Lu	0.24	0.23	0.25	0.22	0.35	0.36	0.39	0.42	0.42	0.33	0.44	0.42	0.37	0.35	0.35	0.41	0.45	0.35	0.20	0.06	0.19	
Nb	7.4	6.0	4.2	5.6	13.4	13.6	13.4	13.3	13.3	13.5	12.3	13.2	12.7	13.0	13.2	13.5	10.4	6.0	7.4	13.7	5.2	
Nd	11.7	12.6	10.0	10.9	33.1	31.1	30.5	32.2	27.4	24.4	30.2	31.9	33.1	33.5	31.1	35.1	25.8	7.7	5.4	12.5	4.9	
Ni	43	28	111	48	17	14	16	20	13	15	18	23	16	21	20	11	nd	nd	nd	nd	nd	
Pr	3.1	3.3	2.4	2.9	9.0	8.5	8.5	8.7	7.2	6.6	8.3	8.6	8.9	8.9	8.3	9.4	7.0	2.3	1.6	3.3	1.5	
Rb	70	45	23	35	167	140	149	141	147	152	151	143	132	130	148	148	151	138	174	166	236	
Sm	2.5	2.6	2.4	2.3	6.7	6.4	6.1	6.5	5.6	5.0	6.2	6.5	6.6	6.7	6.3	7.1	5.6	1.9	1.4	3.4	1.2	
Sn	1	1	1	1	6	3	3	3	3	3	3	3	3	3	4	3	2	5	6	3	5	
Sr	99	153	136	126	121	140	153	124	134	167	125	126	134	138	124	136	107	42	35	146	29	
Ta	0.4	0.4	0.3	0.4	1.1	1.0	1.1	1.0	1.0	1.0	1.1	1.1	1.1	1.0	1.0	1.0	0.8	1.2	2.1	1.3	1.5	
Tb	0.40	0.42	0.43	0.37	0.90	0.83	0.87	0.94	0.87	0.67	0.95	0.91	0.92	0.89	0.91	1.01	0.93	0.45	0.29	0.33	0.27	
Th	3.8	4.2	2.5	4.2	15.1	13.3	14.4	14.3	13.1	13.0	13.9	14.8	15.2	13.5	13.3	15.3	11.8	8.4	6.2	5.6	5.0	
Tm	0.25	0.22	0.26	0.20	0.36	0.36	0.39	0.45	0.42	0.31	0.45	0.43	0.39	0.37	0.38	0.47	0.47	0.34	0.18	0.07	0.18	
U	0.85	0.85	0.53	0.66	1.84	1.63	1.95	3.22	2.58	1.36	3.19	1.89	1.81	1.67	1.98	2.11	1.64	2.36	1.44	0.91	1.63	
V	283	231	296	265	72	67	66	89	66	82	78	92	76	85	84	93	62	8	8	6	6	
W	1	1	1	1	3	2	2	3	2	3	1	1	1	1	5	2	1	1	1	4	3	
Y	13.5	12.6	13.6	12.5	23.7	23.2	25.4	27.1	26.0	18.5	29.6	26.2	26.5	23.1	23.4	28.1	29.3	18.7	10.4	5.5	10.2	
Yb	1.62	1.52	1.61	1.53	2.33	2.48	2.51	2.79	2.86	2.24	2.92	2.81	2.49	2.26	2.38	2.77	3.02	2.35	1.31	0.41	1.34	
Zn	107	139	81	139	102	90	80	132	94	86	81	83	73	90	82	88	73	17	86	24	97	
Zr	48	56	82	54	197	180	171	191	168	181	191	210	198	179	182	180	148	44	30	60	31	
Eu/Eu*	0.81	0.99	0.77	0.89	0.47	0.53	0.53	0.51	0.57	0.64	0.55	0.54	0.53	0.57	0.55	0.54	0.53	0.46	0.46	0.82	0.32	

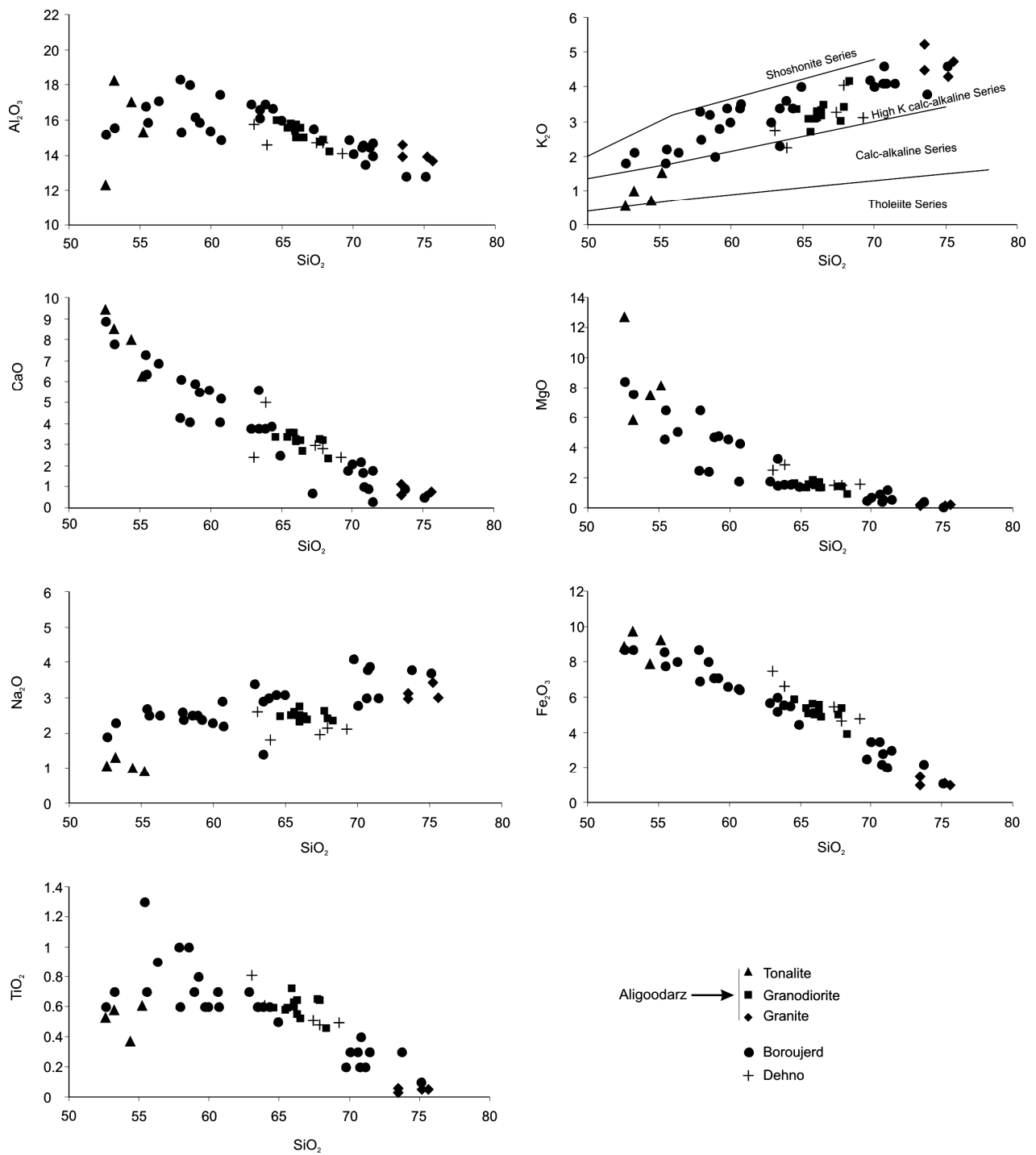


Figure 4: Major elements in Harker plots for the Aligoodarz, Dehno and Boroujerd granitoids. Chemical data for the Dehno and Boroujerd rocks are from Rajaieh (2005) and Ahmadi Khalaji (2007), respectively. The fields of different magma suites in K₂O vs. SiO₂ diagram is after Peccerillo & Taylor (1976).

Figure 10 demonstrates the spider diagrams for different rock types of Aligoodarz, that have been normalized to primordial mantle according to the standard values of Wood *et al.*, (1979). These rocks are predominantly enriched in

Large Ion Lithophile Elements (LILE) such as K, Rb, Th and Cs relative to High Field Strength Elements (HFSE) such as Ta, Nb, Hf, Zr and Ti. They are also enriched in LREE relative to HREE.

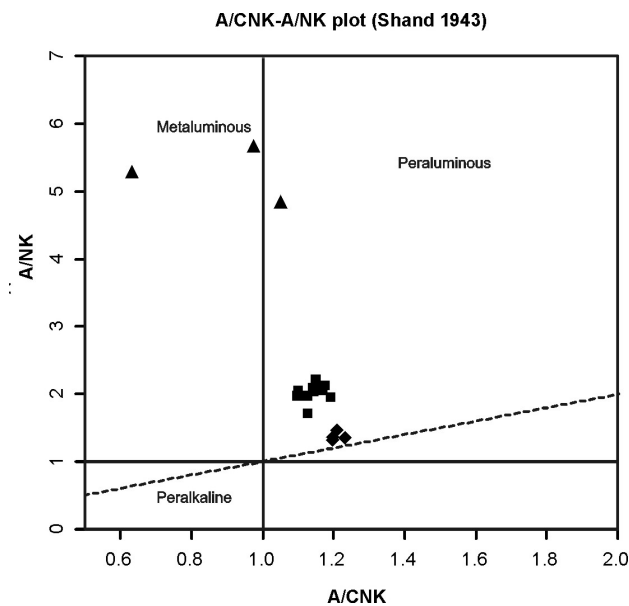


Figure 5: A/NK vs. A/CNK diagram of Shand (1943) discriminating metaluminous, peraluminous and peralkaline compositions. Symbols as in Fig. 4

Discussion

Comparison of chemical data from different plutons of this study indicate that these plutons are genetically linked. Among all the studied rocks, Aligoodarz granitoid represent typical example because Aligoodarz samples range from the most mafic to the most felsic compositions. Generally rocks of other plutons follow the chemical trend of those in Aligoodarz (Figs. 4 and 6). So, petrogenetic properties of the Aligoodarz rocks can clarify some characteristics of the other plutons. In the following we discuss the genesis of Aligoodarz plutons and their link to the ones in other areas.

The main evolving process

Several lines of evidence indicate that fractional crystallization is at least one of the important processes in chemical evolution of granitoids. TiO_2 , Fe_2O_3 , CaO , Al_2O_3 , MgO , Co , V , Cr , and Ni decrease with increasing SiO_2 (Figs. 4 and 6) which is consistent with fractional crystallization of amphibole, biotite, plagioclase and Fe-Ti oxides. Increasing the content of incompatible oxides/elements such as K_2O , Na_2O and Rb with increasing SiO_2 is also consistent with late-stage fractionation of

minerals like K-feldspar and more Na-rich plagioclases.

The REE variations in the Aligoodarz granitoid support the effect of fractional crystallization. It seems that amphibole fractionation has controlled the concave-upward shape of the REE patterns in residual melts and partial differentiation of LREE from HREE (Gromet and Silver, 1983; Sawka & Chappell, 1988; and Romick *et al.*, 1992). The increase in Eu anomaly from tonalite to granodiorite and granite (Fig. 8) is in accord with the progressive removal of plagioclase from the magma.

Zr is an important element in evaluating the process that involved in magma evolution (e.g. Chappell, 1996). An inflection occurs in Zr- SiO_2 diagram (Fig. 6) when SiO_2 reaches at about 66 wt%. This behavior is consistent with concentration of Zr that increases from tonalite to granodiorite, indicating a Zr-undersaturated melt for tonalite. This is characteristic of melts in which variation is mainly controlled by fractional crystallization process (Chappell, 1996). It seems that at SiO_2 content of ~66 wt%, when the melt became oversaturated in Zr, zircon started to crystallize and thus Zr concentration dropped rapidly in the remaining melt as evidenced from lower concentration of Zr in the granite and the presence of abundant zircon grains in the granodiorite samples.

Accessory minerals typically compose less than one modal percent of a whole-rock sample, yet host significant fractions of the whole-rock budget of important trace elements (Gromet and Silver, 1983; Bea, 1996; Vervoot *et al.*, 1996). Zircon is an accessory mineral which is one of the main hosts of REE (e.g. Gromet and Silver, 1983; Le Marchand *et al.*, 1987; Yurimoto *et al.*, 1990; Bea, 1996; Vervoot *et al.*, 1996). So, high positive correlation between Zr and $\sum\text{REE}$ (Fig. 11) suggest that zircon is the main host of REE and indicates the role of zircon fractionation on REE enrichment of the granitoids.

Although the above mentioned evidence support the role of fractional crystallization, more detailed investigations are necessary to

examine the role of other processes. Esna-Ashari *et al.*, (2011) showed that variation trends of Aligoodarz granitoids cannot be generated by magma mixing. However the role

of assimilation of country rocks partial melts might be an important process that cannot be investigated by the available data presented in this paper.

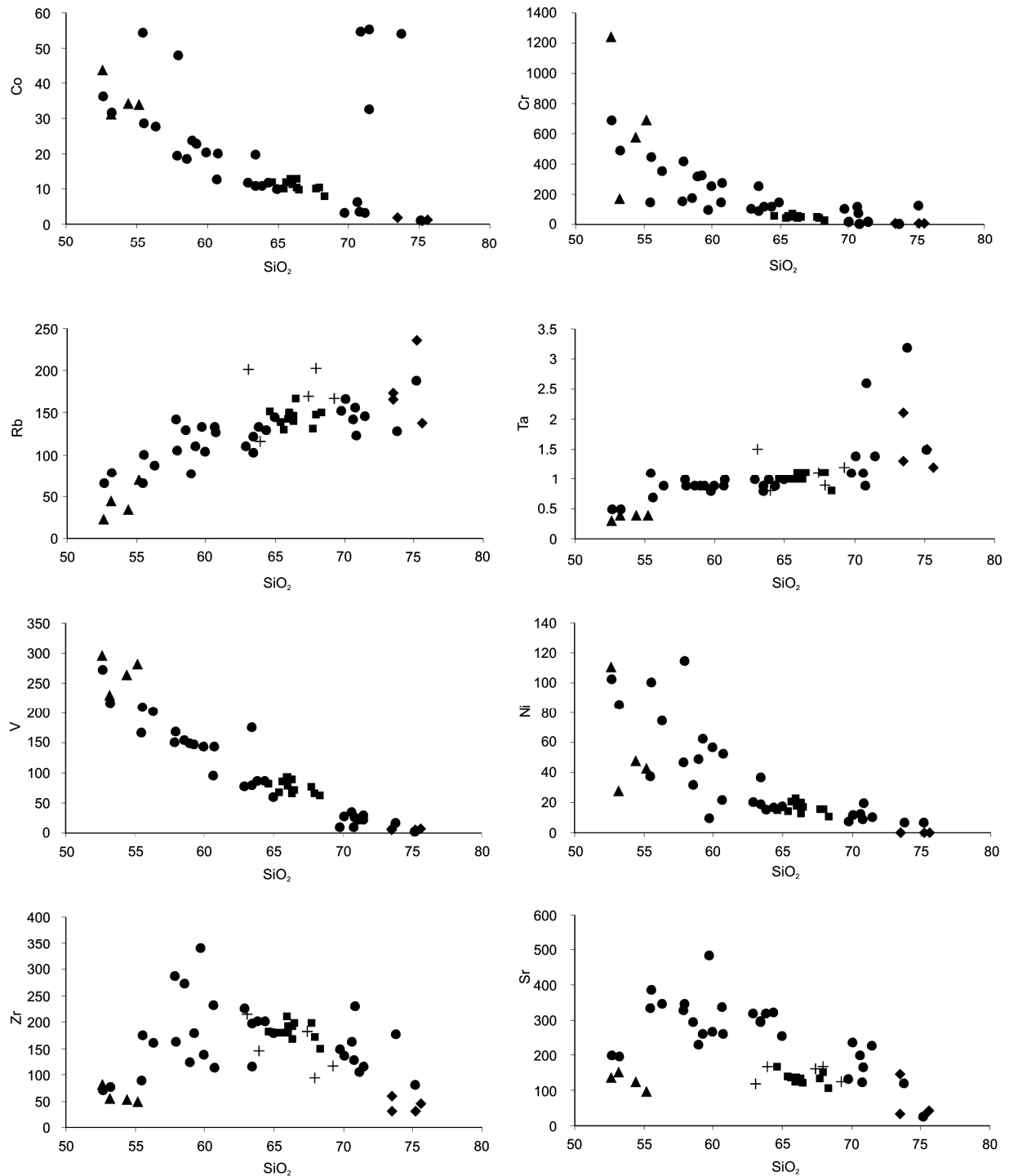


Figure 6: Trace elements in Harker plots for the Aligoodarz, Dehno and Boroujerd granitoids. Chemical data for the Dehno and Boroujerd rocks are from Rajaieh (2005) and Ahmadi Khalaji (2007), respectively. Because Co, Cr, V and Ni are not reported by Rajaieh (2005), the Dehno rocks are not plotted on the corresponding diagrams. Symbols as in Figure 4.

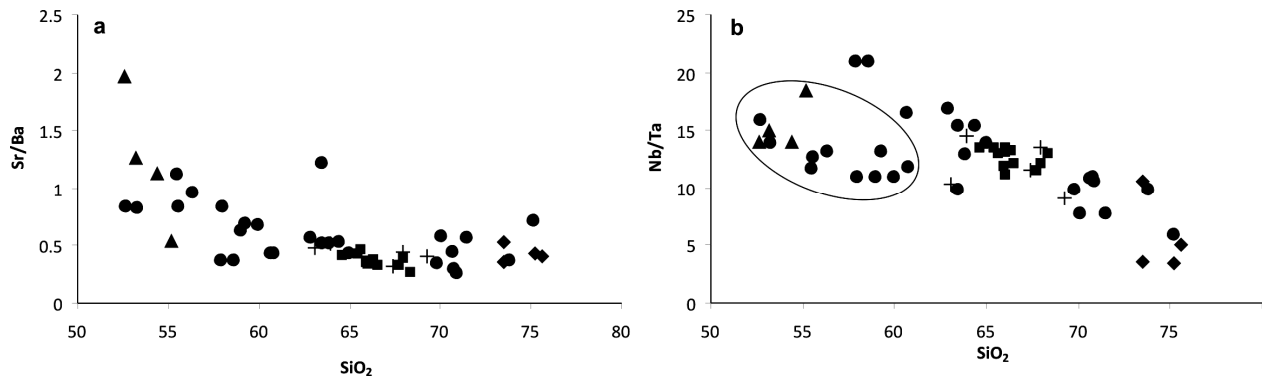


Figure 7: (a) Sr/Ba vs. SiO₂ diagram. For samples having less than ~68 wt% SiO₂, the ratio of Sr/Ba decreases with increasing SiO₂. This ratio slightly increases if SiO₂ content exceed 68 wt%. (b) Nb/Ta vs. SiO₂ diagram. All the analysed samples show decreasing trend of Nb/Ta with increasing SiO₂. Intermediate rocks (tonalities) which are surrounded by an ellipsoid, are showing different trend from the felsic rocks (granodiorite + granite). Symbols as in Figure 4.

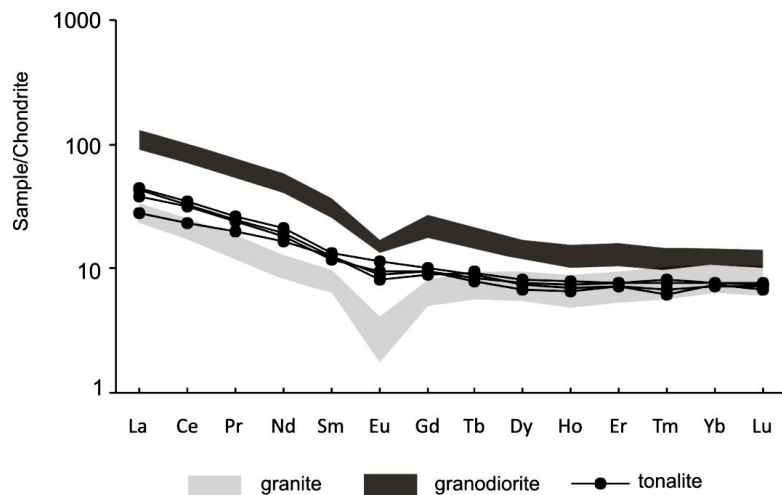


Figure 8: Chondrite normalized REE patterns of tonalite, granodiorite and granite of the Aligoodarz (chondrite values from Boynton, 1984).

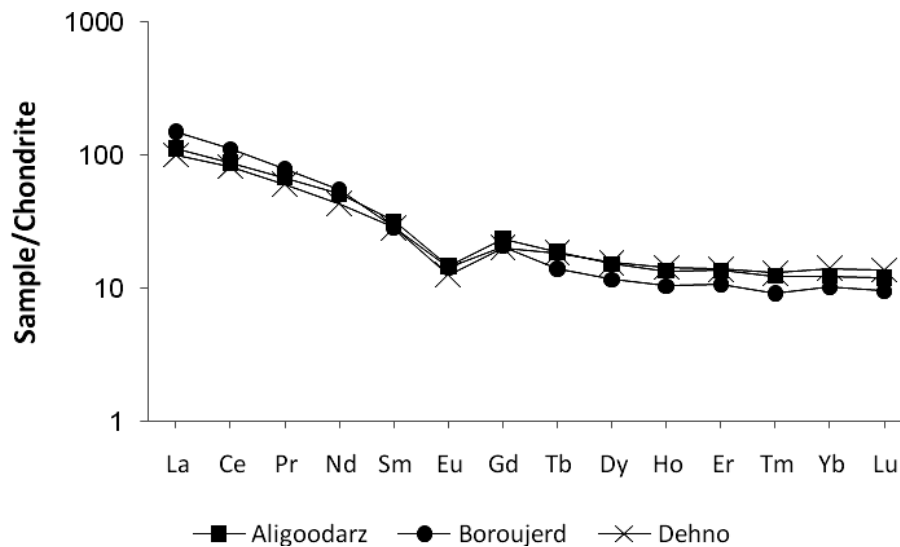


Figure 9: Chondrite normalized REE patterns for average composition of Aligoodarz, Dehno and Boroujerd granodiorites (chondrite values from Boynton, 1984).

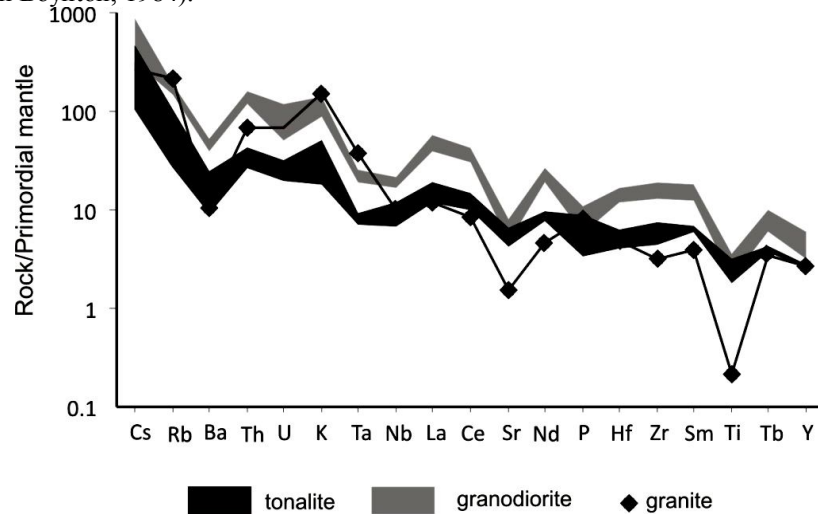


Figure 10: Multi-element patterns (spider diagrams) for the Aligoodarz granitoid. The plot for granite samples is based on the average calculated for four analyses. The normalized values are from Wood *et al.*, (1979)

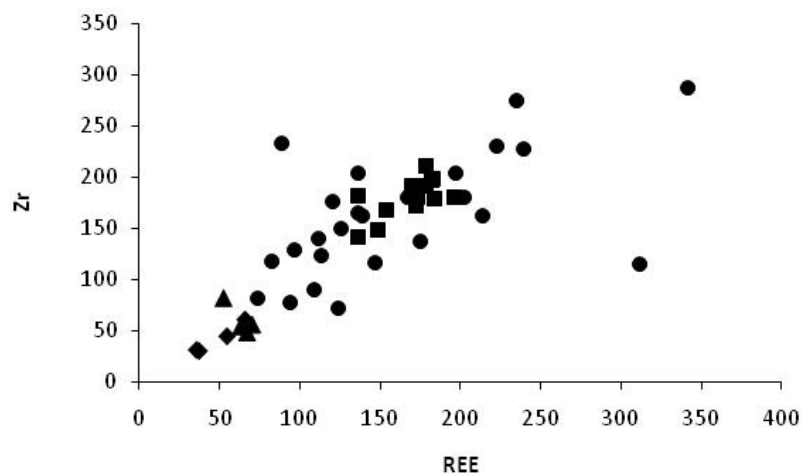


Figure 11: Zr vs. Σ REE variation diagram for the Aligoodarz, Dehno and Boroujerd granitoids (symbols as in Fig. 4)

Different behavior of intermediate rocks

For all the studied rocks, samples with lower silica content show scattered patterns (Figs 4 and 6) in some variation diagrams (e.g. plots of TiO_2 , Al_2O_3 , Cr, Ni and Sr vs. SiO_2). In previous studies such behavior of intermediate samples was attributed to their different source or different magmatic processes (Ahmadi Khalaji *et al.*, 2007). In the following statements it can be seen that the abundance of some minerals in these samples is different and this is the cause of their different chemical behavior.

On the Al_2O_3 and MgO vs. SiO_2 plots (Fig. 4), the Aligoodarz tonalites show a significant difference in the contents of Al_2O_3 and MgO.

Microscopic studies of the Aligoodarz tonalites indicate that these chemical differences can be generated by variation in modal abundances of plagioclase and amphibole, leading to higher values in MgO, Cr and Ni where amphibole is dominated but higher Al_2O_3 where plagioclase is abundant. Significant variation for CaO concentration is not observed because Ca can easily enter in both amphibole and plagioclase. Tonalite samples from Boroujerd which are relatively similar in silica values with those of the Aligoodarz tonalites, have relatively lower modal content of amphibole but higher content of plagioclase. Lower ability of Sr for substitution in amphibole structure but its higher ability for substitution in plagioclase led to

Aligoodarz tonalites being depleted in Sr (Fig. 6). Two samples of Boroujerd which plot close to the Aligoodarz tonalites have higher abundance of amphibole in comparison with other samples of Boroujerd (Ahmadi Khalaji, 2006). Also, in variation diagrams of Zr and Ta vs. SiO₂ these two samples plot close to the Aligoodarz tonalites. Since amphibole can have an important role on Ta depletion (e.g. Tiepolo *et al.*, 2000) and zircon on Zr enrichment, higher content of amphibole and probably lower content of zircon in these two samples correspond to respectively lower Ta and Zr concentrations. This supports the relevant interpretations for effect of mineral frequency in chemical behavior of intermediate rocks.

Differences in modal content of minerals (table 1) and consequent differences in chemical variation of intermediate rocks is also evident in Sr/Ba vs. SiO₂ diagram (Fig. 7). Four samples of Aligoodarz tonalite, although having relatively similar abundance of SiO₂, are characterized by very different Sr/Ba ratios. Sr readily participates in plagioclase structure and Ba in biotite during crystal fractionation. Variation in plagioclase and biotite contents of these samples can produce scattering because there is a correlation between Sr/Ba and plagioclase/biotite ratios. Although Sr/Ba variation in the samples with lower silica content is not linear, they show a general decreasing trend. This is consistent with the studies of Hanson (1978) as fractionation of plagioclase leads to low Sr/Ba ratio in the remaining melt. This ratio slightly increases as the SiO₂ content exceeds ~68 wt%. Fractionation of biotite and Ba depletion in the remaining melt can be considered as the cause of such increasing trend observed in the felsic samples.

In many co-magmatic suites the ratio of Nb/Ta varies from mafic to felsic rocks indicating fractionation of Nb from Ta in silicate melts during fractional crystallization (e.g. Linnen and Keppler, 1997; Tiepolo *et al.*, 2000; Schmidt *et al.*, 2004). Amphibole (Tiepolo *et al.*, 2000), Ti-bearing minerals (e.g. titanite) and rutile

(Linnen & Keppler, 1997; Green, 1995) are important minerals that can fractionate Nb from Ta. Thus, regarding the Nb/Ta variation in Fig. 7, distinct varied trends between intermediate and felsic rocks may be the result of 1- presence of amphibole in just intermediate rocks; 2- significant effect of rutile in Nb/Ta fractionation in just felsic rocks because rutile is an important minor mineral which prefer Nb over Ta in just peraluminous granitic melts (Linnen & Keppler, 1997).

Tectonic setting

Trace element discrimination diagrams have been used as a means of fingerprinting the tectonic environments in the formation of granitoids. The Aligoodarz granitoid plots in the volcanic arc granite field in both the Rb vs. Y+Nb and Ta vs. Yb discrimination diagrams (Fig. 12) of Pearce *et al.*, (1984) consistent with the tectonomagmatic setting proposed for the SSZ. Only samples from granites, shift toward the syncollision field. This is characteristic of chemical affinity of syncollision peraluminous granites with highly fractionated volcanic-arc magmas (e.g. Harris *et al.*, 1986).

Since the early days of plate tectonics, the South American Andes have been cited as a type example of an ocean-continent subduction zone, or active continental margin (e.g. Mitchell & Reading 1969). By using geochemical data from south American Andes and some other collisional zones from different areas of the earth, Brown *et al.*, (1984) distinguished three types of granitoid-bearing arcs (Fig. 13a): i) the primitive island and continental arcs (M-type category of calcic, metaluminous granitoids); (ii) the normal continental arcs which are abundant I-type calc-alkaline metaluminous to peraluminous suites; and (iii) the mature continental arcs that often form S-type granites. Comparing the data with the field of arc-type granitoids (Fig.13a); the Aligoodarz, Dehno and Boroujerd rocks plot mainly in the field of normal continental arcs. Spider diagrams of granodiorites of this study are also comparable with those of I-type granitoids formed in normal

continental arcs (Fig. 13b). Marked Nb-Ta trough and Cs-enrichment relative to Rb and K (Figs. 10 and 13b) are the most persistent features of the spider diagrams of volcanic arc rocks, which is probably due to different proportion of retention of these elements in the source during partial melting of the subducted oceanic crust (Wilson, 1989; Hart & Reid 1991; Pearce and Peate, 1995; Elliott *et al.*, 1997). In general, enrichment in LREE and LILE relative to HREE and HFSE in the studied rocks are typical features of calc-alkaline magmatism in subduction related environments (e.g. Cox *et al.*, 1973, 1979).

Moazzen *et al.*, (2004) stated that the

Mollataleb granitoid (Fig. 1d) generated from S-type source regions in which magmas can produce in syncollisional tectonic setting due to the collision of Afro-Arabian continental plate and the CIP, the present study however do not confirm this scenario (see also the following section). Except few samples, all the obtained analyses of this study fall within the volcanic arc (Fig. 12), whereas, Moazzen *et al.*, (2004) inferred a syncollisional tectonic setting. Such controversy may be related to inappropriate sampling, analytical accuracies and degree of alteration as evidenced from lower Na₂O content of samples from Mollataleb granitoid, provided by Moazzen *et al.*, (2004).

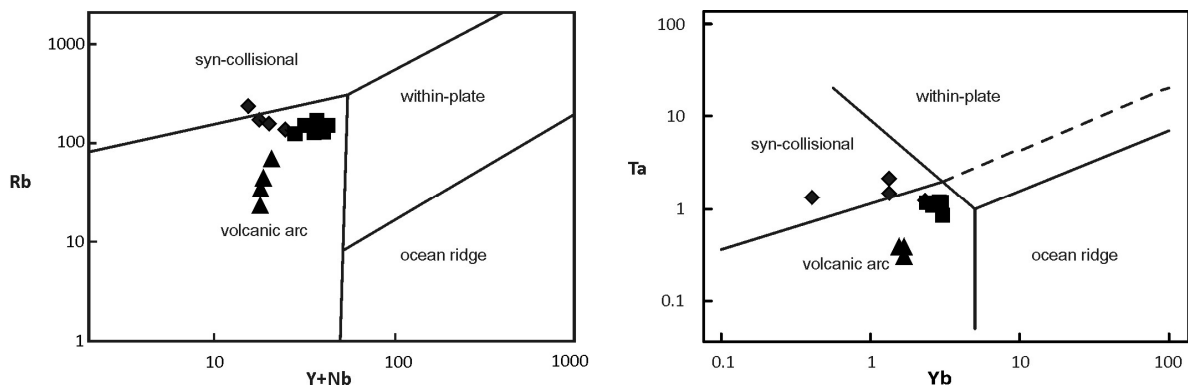


Figure 12: Trace element discrimination diagrams of Pearce *et al.*, (1984). Symbols as in Figure 4

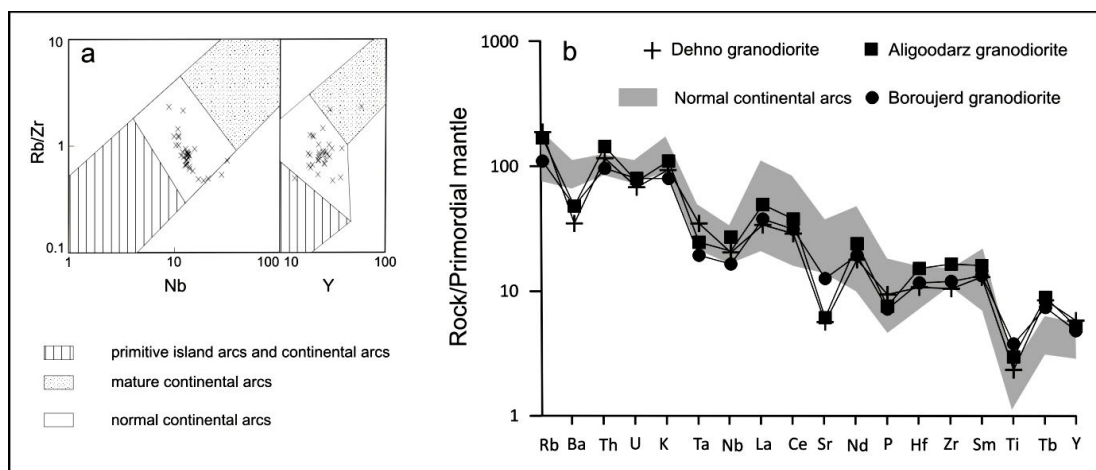


Figure 13: Comparison of the Aligoodarz, Dehno and Boroujerd granitoids with Mesozoic and Cenozoic magmatic arcs (after: Brown *et al.*, 1984); a) Plots of Rb/Zr against Nb and Y; b) Primordial mantle-normalized trace element patterns of Aligoodarz, Boroujerd and Dehno granodiorites and the granitoids of normal continental arcs in the SiO₂ range 66-75 wt%. Since granodiorite is the main rock type in the study area, they are shown in the plot.

Petrogenetic consideration

All major and trace elements and also multi-element patterns of Aligoodarz granitoid are comparable to those of Dehno and Broujerd

suggesting that the studied rocks are possibly related to and most likely derived from the same parental melt. Hence, different rock types taken from whole areas under this study can be

considered as a simple suite in which magmas are co-genetic.

Most geochemical variations of this suite is linear (Figs. 4 and 6), but there are deviations at the mafic ends for some elements (Al_2O_3 , MgO , TiO_2 , Cr, Ni and Sr). It is noticeable that when there is a scattered pattern in the intermediate samples of Aligoodarz, there is the same scattering in the similar samples from Boroujerd (e.g. TiO_2 in Fig. 4; Cr, Zr and Sr in Fig. 6). This similarity supports the co-genetic relation of the rocks in Aligoodarz and Boroujerd areas (White *et al.*, 2001). However the main chemical differences between the rocks of these areas are lower abundance of Na_2O , K_2O , Ba and Sr in the Aligoodarz and Dehno samples relative to those in Boroujerd. The lack of alkali elements (Na and K) has caused an increase in A/CNK or ASI values for the Aligoodarz and Dehno samples. Late stage hydrothermal alteration (e.g. Zen, 1988; Chappell & White, 1992) and/or assimilation of sedimentary rocks (e.g. DePaolo, 1981) can explain the lower abundance of above elements and consequently higher ASI values of the Aligoodarz and Dehno granitoids. However, high correlations that are shown in Figures 4 and 6 indicate that the assimilation and/or late stage hydrothermal alteration was not extensive.

The co-genetic relation for the studied granitoids is also shown on the $\text{Al}_2\text{O}_3/\text{TiO}_2$ vs. TiO_2 diagram where they display one curvilinear trend (Fig. 14). Garcia *et al.*, (1994) demonstrated that $\text{Al}_2\text{O}_3/\text{TiO}_2$ is readily modified during magmatic differentiation and it can discriminate between the fractional crystallization and restite models. On the $\text{Al}_2\text{O}_3/\text{TiO}_2$ vs. TiO_2 diagram (Fig. 14), this suite displays a curved trend, typical of magmatic differentiation, thus cannot be the result of restite fractionation. However, due to the large area of exposure of different types of granitoids in different locations, magmatic differentiation need to be considered with some cautious as the only process of magma evolution.

The co-genetic relation of the granitoids is also

supported by similarities in their crystallization age. The U-Pb zircon dating of Aligoodarz granitoid (~178 Ma) determined by Esna-Ashari *et al.*, (2009) is very similar to the age of Boroujerd granitoids (170 Ma) obtained by Ahmadi Khalaji (2006), all indications of synchronous plutonism occurred in Middle Jurassic times. This together with similarities in geochemical signatures indicate a close genetic relation for the studied rocks.

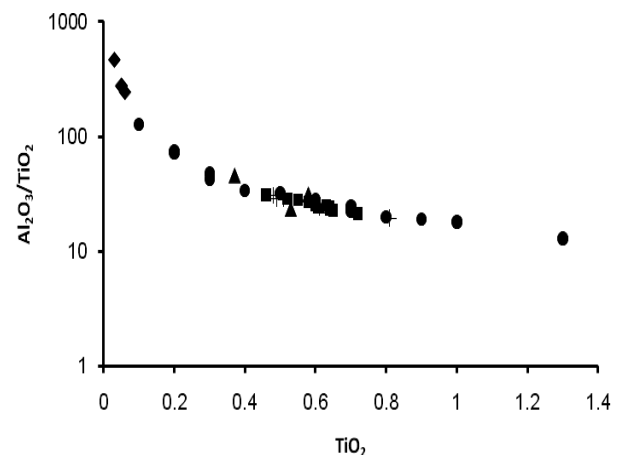


Figure 14: $\text{Al}_2\text{O}_3/\text{TiO}_2$ vs. TiO_2 diagram for the investigated granitoid suite showing one curvilinear trend for the all plutonic rocks of the Aligoodarz, Dehno and Boroujerd areas, illustrating typical of magmatic differentiation. Symbols as in Figure 4.

In the AFM diagram of Beard (1986), major element composition of the tonalites are compared with the well-known arc related mafic cumulates and mafic non-cumulate rocks (Fig. 15). The Aligoodarz tonalites plot in the field of mafic cumulates. This can imply cumulate nature of the tonalites, consistent with the presence of disrupted fragments of Aligoodarz tonalites as mafic enclaves within the adjacent granodiorites that indicates earlier crystallization of tonalites (Fig. 2a). The Boroujerd tonalites don't plot in the cumulate fields of Figure 15. They are compositionally between mafic cumulates and felsic rocks and plot close to the non-cumulate mafic field. This implies that Boroujerd tonalites have more evolved compositions and are characterized by less abundant primary accumulated minerals but higher proportion of evolved melt. A cumulate

origin for the tonalites is also suggested in Figure 16, which presents the results of fractionation modeling of Sr, Rb and Ba (Roberts *et al.*, 2000). In these diagrams, the Sr, Rb and Ba contents of tonalites could be explained by the accumulation of amphibole from a mafic magma. Feldspar fractionation can also explain the negative gradient of the data through the felsic rocks.

Source material of granitoids and also the crustal depth in which the magma is crystallized are the two main subjects in the petrogenesis of igneous rocks. Regarding the granitoids of this study, relative depletion of Ta and Nb (Brown *et al.*, 1984), high concentration of LILE and LREE (Brown *et al.*, 1984; Pearce & Peate, 1995) and low concentration of Ti and P (Taylor & McLennant, 1985), are all typical criteria of rock generation from continental crustal materials. Source of heat for crustal melting probably was from mantle-derived magma. Subduction of oceanic crust is accompanied by dehydration and perhaps melting of the subducted crust, leading to melting of the mantle wedge above the subducted slab. Magmas generated in the mantle wedge or subducting slab must traverse the thick layer of sialic and incompatible

element-enriched crust before reaching the surface. So, noticeable crustal contamination can take place at this step. Aligoodarz tonalites are the least evolved granitoid rocks. In K_2O vs. SiO_2 discrimination diagram of Fig. 4 they plot in series with lower K_2O content but they don't show the mantle affinities. Probably the original magma highly contaminated by crustal derived melts and became very similar to crustal melts before reaching the surface.

I-type nature of the Boroujerd granitoid is identified by Ahmadi Khalaji *et al.*, (2007). These rocks have $(^{87}Sr/^{86}Sr)_i$ and $(^{143}Nd/^{144}Nd)_i$ ratios vary from 0.7062 to 0.7074 and 0.51223 to 0.51226, respectively characteristic of typical I-type granites with lower crustal signature. Accordingly, the same source can be considered for the Aligoodarz and Dehno granitoids. Also low abundances of surmicaceous enclaves, in addition to wide range of SiO_2 content (52-75 wt%) are the features confirming the I-type nature of the Aligoodarz granitoid (e.g. Chappell & White, 1974 and 1992). The source region of magma generation was not in deep crustal levels because REE fractionation is relatively moderate for all the studied rocks (Fig. 8), suggest a garnet-free source material and relatively low pressure conditions.

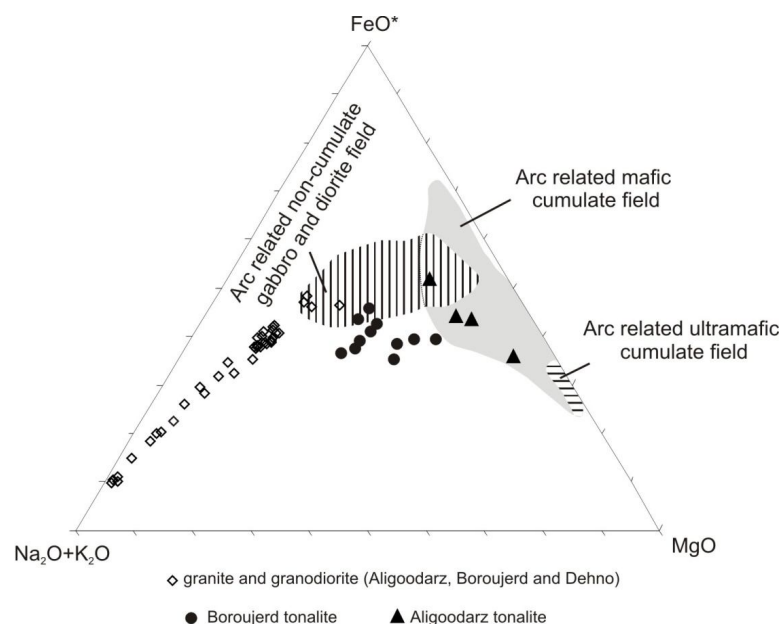


Figure 15: AFM compositions of the studied samples. Fields of cumulate and non-cumulate rocks are from Beard (1986).

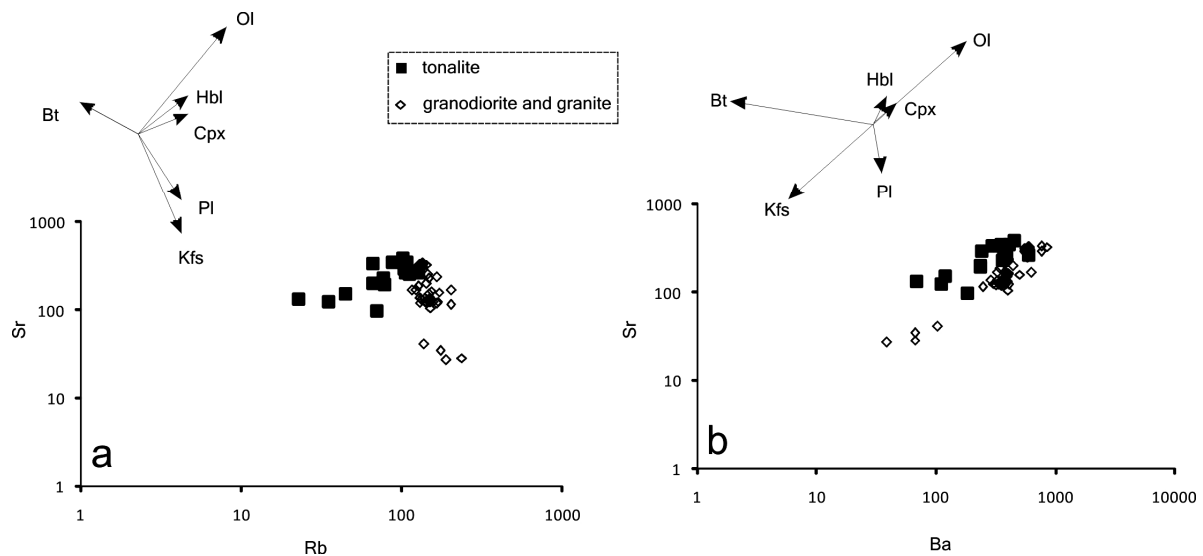


Figure 16: Plots of Sr vs. Rb (a), and Sr vs. Ba (b) for the granitoids of Aligoodarz, Boroujerd and Dehno areas. Fractional crystallization vectors are after Roberts *et al.*, (2000).

Conclusions

The Aligoodarz granitoid consists of three rock types including tonalite, granodiorite and granite. Microscopic observations and whole rock geochemical indications for the Aligoodarz samples are very similar to those of the Dehno and Boroujerd granitoids. Similar variation trends in the Harker diagrams and their close association in space and time confirm synchronous plutonism with a similar source material. Fractional crystallization is the main evolving mechanism and rocks with higher color index resulted from mineral accumulation of a more mafic precursor. Granitoids of this study have chemical indications representing normal I-type characteristics. They represent features

that indicate formation of magma in continental arc environment. They have strong evidence that reveals contribution of continental crust in their generation. The heat source for melting the continental crust was from subduction related magmatism in an active continental margin. Formation of these granitoids is related to subduction of Neotethyan oceanic lithosphere below the CIP.

Acknowledgments

This study was financially supported by the Iran National Science Foundation (INSF), Grant no. 87020210. University of Tehran is also acknowledged for preparing suitable environment and facilities for this research.

References

- Ahmadi Khalaji, A., 2006. Petrology of the granitoid rocks of the Boroujerd area. Ph.D Thesis, University of Tehran, Tehran, Islamic Republic of Iran.
- Ahmadi Khalaji, A.A., Esmaily, D., Valizadeh, M.V., Rahimpour-Bonab, H., 2007. Petrology and geochemistry of the granitoid complex of Boroujerd, Sanandaj- Sirjan Zone, Western Iran. *Journal of Asian Earth sciences*, 29 859-877.
- Alavi, M., 1980. Tectonostratigraphic evolution of the Zagrosides of Iran. *Geology*, 8 144-149.
- Alavi, M., 1991. Tectonic map of the Middle East. Geological Survey of Iran, scale 1:2,900,000.
- Alavi, M., 1994. Tectonic of the Zagros orogenic belt of Iran: new data and interpretations. *Tectonophysics*, 229 211-238.
- Alavi, M., 2004. Regional stratigraphy of the Zagros fold-thrust belt of Iran and its proforeland evolution. *American Journal of Science*, 304 1-20.
- Arvin, M., Pan, Y., Dargahi, S., Malekizadeh, A., Babaei, A., 2007. Petrochemistry of the Siah-Kuh granitoid stock southwest of Kerman, Iran: Implications for initiation of Neotethys subduction. *Journal of Asian Earth Sciences*, 30 474-489.

- Bea, F., 1996. Residence of REE, Y, Th and U in granites and crustal protoliths; implications for the chemistry of crustal melts. *Journal of petrology*, 37 521-552.
- Beard, J.S., 1986. Characteristic mineralogy of arc-related cumulate gabbros: implications for the tectonic setting of gabbroic plutons and for andesite genesis. *Geology*, 14 848– 851.
- Berberian, F., Berberian, M., 1981. Tectono-plutonic episodes in Iran. In: Gupta, H.K., Delany, F.M. (Eds.), *Zagros Hindukush, Himalaya Geodynamic Evolution*. American Geophysical Union, Washington, DC, pp. 5–32.
- Berberian, M., 1995. Master "blind" thrust faults hidden under the Zagros folds: active basement tectonics and surface morphotectonics. *Tectonophysics*, 241 193-224.
- Berberian, M., King, G.C.P., 1981. Towards a paleogeography and tectonic evolution of Iran. *Canadian Journal of Earth Science*, 18 210–265.
- Boynnton, W.V., 1984. Cosmochemistry of the rare earth elements: meteorite studies. In: Henderson P. (Ed.), *Rare earth element geochemistry*. Elsevier, 63-114.
- Brown, G.C., Thorpe, R. S., Webb, P. C., 1984. The geochemical characteristics of granitoids in contrasting arcs and comments on magma sources. *Journal of the Geological Society*, 141 413-426.
- Chappell, B.W., 1996. Compositional variation within granite suites of the Lachlan Fold Belt: its causes and implications for the physical state of granite magma. *Transactions of the Royal Society of Edinburgh: Earth Sciences*, 88 159-170.
- Chappell, B.W., White, A.J.R., 1974. Two contrasting granite types. *Pacific Geology*, 8 173–174.
- Chappell, B.W., White, A.J.R., 1992. I and S-type granites in the Lachlan Fold Belt. *Transactions of the Royal Society of Edinburgh: Earth Sciences*, 83 1–26.
- Cox, D.P., Schmidt, R.G., Vine, J.D., Kirkemo, H., Tourtelot, E., Fleischer, M., 1973. Copper, In: Brobst, D.A., Pratt, W.P. (Eds.), *United States Mineral Resources*. US, Geological Survey Professional Paper 820, pp. 163–190.
- Cox, K.G., Bell, J.D., Pankhurst, R.J., 1979. *The Interpretation of Igneous Rocks*. George Allen & Unwin, London.
- DePaolo, D.J., 1981. Trace element and isotopic effects of combined wallrock assimilation and fractional crystallization. *Earth and Planetary Science Letters*, 53 189-202.
- Dercourt, J., Zonenshain, L.P., Ricou, L.-E., Kazmin, V.G., Le Pichon, X., Knipper, A.L., Grandjacquet, C., Sbertshikov, I.M., Geysant, J., Lepvrier, C., Pechersky, D.H., Boulin, J. Sibuet, J.-C. Savostin, L.A., Sorokhtin, O., Westphal, M., Bazhenov, M.L., Lauer, J.P., Biju-Duval, B., 1986. Geological evolution of the Tethys belt from the Atlantic to Pamirs since the Lias. *Tectonophysics*, 123 241–315.
- Elliott, T., Plank, T., Zindler, A., White, W. & Bourdon, B. 1997. Element transport from subducted slab to volcanic front at the Mariana arc. *Journal of Geophysical Research*, 102 14991–15019.
- Esna-Ashari, A., Hassanzadeh, J., Valizadeh, M.V., 2011. Geochemistry of microgranular enclaves in Aligoodarz Jurassic arc pluton, western Iran: implications for enclave generation by rapid crystallization of cogenetic granitoid magma. *Mineralogy and Petrology*, 101 195-216.
- Esna-Ashari, A., Hassanzadeh, J., Wernicke, B.P., Achmitt, A.K., Axen, G., Horton, B., 2009. Middle Jurassic flare-up and cretaceous magmatic lull in the central Sanandaj-Sirjan arc, Iran: analogy with the southwestern United States. *GSA Annual Meeting (18-21 October 2009)*.
- Garcia, D., Fontelles, M., Moutte, J., 1994. Sedimentary fractionation between Al, Ti, and Zr and the genesis of strongly peraluminous granites. *The Journal of Geology*, 102 411–422.
- Golonka, J., 2000. *Cambrian–Neogen Plate Tectonic Maps*. Wydawnictwo Uniwersytetu Jagiellońskiego, Kraków, Poland. 125 p.
- Green, T.H., 1995. Significance of Nb/Ta as an indicator of geochemical processes in the crust-mantle system. *Chemical Geology*, 120 347-359.
- Gromet, L.P., Silver, L.T. 1983. Rare earth element distributions among minerals in a granodiorite and their petrogenetic implications. *Geochimica et Cosmochimica Acta*, 47 925-939.
- Hanson, G.N., 1978. The application of trace elements to the petrogenesis of igneous rocks of granitic composition. *Earth and planetary science letters*, 38 26-43.
- Harris, N.B.W., Pearce, J.A., Tindle, A.G., 1986. Geochemical characteristics of collision-zone magmatism. In: Coward, M.P., Ries, A.C. (Eds.), *Collision Tectonics*. Geological Society London, Special Publication 19, pp. 67–81.
- Hart, S.R., Reid, M.R., 1991. Rb/Cs fractionation: a link between granulite metamorphism and the S-process. *Geochimica et Cosmochimica Acta*, 55 2379-2383.
- Hassanzadeh, J., Stockli, D.F., Horton, B.K., Axen, G.J., Stockli, L.D., Grove, M., Schmitt, A.K., Walker, J.D., 2008. U-Pb zircon geochronology of late Neoproterozoic–Early Cambrian granitoids in Iran: Implications for paleogeography, magmatism, and exhumation history of Iranian basement. *Tectonophysics*, 451 71-96.
- Heydari, E., 2008. Tectonics versus eustatic control on supersequences of the Zagros Mountains of Iran. *Tectonophysics*, 451 56-70.

- Hooper, R.J., Baron, I., Hatcher Jr., R.D., Agah, S., 1994. The development of the southern Tethyan margin in Iran after the break up of Gondwana: implications of the Zagros hydrocarbon province. *Geosciences*, 4 72–85.
- Kazmin, V.G., 1991. Collision and rifting in the Tethys Ocean: geodynamic implications. *Tectonophysics*, 196 371–384.
- Le Marchand, F., Villemant, B., Calas, G., 1987. Trace element distribution coefficients in alkaline series. *Geochimica et Cosmochimica Acta*, 51 1071–1081.
- Linnen, R.L., Keppler, H., 1997. Columbite solubility in granitic melts: consequences for the enrichment and fractionation of Nb and Ta in the Earth's crust, *Contributions to Mineralogy and Petrology*, 128 213–227.
- Masoudi, F., 1997. Contact metamorphism and pegmatite development in the SW of Arak, Iran. PhD thesis, The University of Leeds, UK, pp. 231.
- Mitchell, A.H., Reading, H.G., 1969. Continental margins, geosynclines and ocean floor spreading. *The Journal of Geology*, 77 629–646.
- Moazzen, M., Moayyed, M., Modjarrad, M., Darvishi, E., 2004. Azna granitoid as an example of syn-collision S-type granitisation in Sanandaj-Sirjan metamorphic belt, Iran. *Neues Jahrbuch für Mineralogie-Monatshefte*, 11 489–507.
- Mohajjel, M., Fergusson, C.L., 2000. Dextral transpression in Late Cretaceous continental collision, Sanandaj-Sirjan Zone, Western Iran. *Journal of Structural Geology*, 22 1125–1139.
- Mohajjel, M., Fergusson, C.L., Sahandi, M.R., 2003. Cretaceous–Tertiary convergence and continental collision, Sanandaj-Sirjan Zone, Western Iran. *Journal of Asian Earth Sciences*, 21 397–412.
- Pearce, J.A., Peate, D.W., 1995. Tectonic implication of the composition of volcanic arc magmas. *Annual Review of Earth and Planetary Sciences* 23, 251–285.
- Pearce, J.A., Harris, N.B.W., Tindle, A.G., 1984. Trace element discrimination diagrams for the tectonic interpretation of granitic rocks. *Journal of Petrology*, 25 956–983.
- Peccerillo, A., Taylor, S.R., 1976. Geochemistry of Eocene calc-alkaline volcanic rocks from the Kastamonu area, Northern Turkey. *Contributions to Mineralogy and Petrology*, 58 63–81.
- Rajaieh, M., 2005. Petrology and geochemistry of the Dehno intrusive rocks (northeast of Aligoodarz. 131pp. M.Sc. thesis (in Persian; University of Isfahan, Iran).
- Roberts, M., Pin, C., Clemens, J.D., Paquette, J-L., 2000. Petrogenesis of mafic to felsic plutonic rock associations: the calc-alkaline Quérigut complex, French Pyrenees. *Journal of Petrology*, 41 809–844.
- Romick, J.D., Kay, S.M., Kay, R.M., 1992. The influence of amphibole fractionation on the evolution of calc-alkaline andesite and dacite tephra from the central Aleutians, Alaska. *Contributions to Mineralogy and Petrology*, 112 101–118.
- Ruttner, A., Stöcklin, J., 1967. Geological map of Iran. Geological Survey of Iran, scale 1:1000,000.
- Sabzehei M., Eshraghi., S., 1995. Geological map of the Neyriz. Geological Survey of Iran, scale 1:100,000.
- Sawka, W.N., Chappell, B.W., 1988. Fractionation of uranium, thorium and rare earth elements in a vertically zoned granodiorite: Implications for heat production distributions in the Sierra Nevada batholith, California, U.S.A. *Geochimica et Cosmochimica Acta*, 52 1131–1143.
- Schmidt, M.W., Dardon, A., Chazot, G., Vannucci, R., 2004. The dependence of Nb and Ta rutile-melt partitioning on melt composition and Nb/Ta fractionation during subduction processes. *Earth and Planetary Science Letters*, 226 415–432.
- Sengör, A.M.C., 1990. A new model for the late Paleozoic–Mesozoic tectonic evolution of Iran and implications for Oman. In: Robertson, A.H.F., Searle, M.P., Ries, A.C. (Eds.). *The Geology and Tectonics of the Oman Region*, Geological Society of London, Special Publication, 22 pp. 278–281.
- Sepahi, A.A., 2008. Typology and petrogenesis of granitic rocks in the Sanandaj-Sirjan metamorphic belt, Iran: with emphasis on the Alvand plutonic complex. *Neues Jahrbuch für Geologie und Palaontologie-Abhandlungen*, 247 295–312.
- Sepahi, A.A., Athari, S. F., 2006. Petrology of major granitic plutons of the northwestern part of the Sanandaj-Sirjan Metamorphic Belt, Zagros Orogen, Iran: with emphasis on A-type granitoids from the SE Saqqez area. *Neues Jahrbuch für Mineralogie-Abhandlungen*, 183 93–106.
- Shabanian, N., Khalili, M., Davoudian, A, R., Mohajjel, M., 2008. Petrography and geochemistry of mylonitic granite from Ghaleh-Dezh, NW Azna, Sanandaj-Sirjan Zone, Iran. *Neues Jahrbuch für Mineralogie-Abhandlungen*, 185 2–16.
- Shand, S.J., 1943. *The eruptive rocks*: 2nd edition, John Wiley, New York, 444 p.
- Stampfli, G., Marcoux, J., Baud, A., 1991. Tethyan margins in space and time. *Palaeogeography, Palaeoclimatology, Palaeoecology*, 87 373–409.
- Taylor, S.R., McLennant, S.M., 1985. *The Continental Crust: Its Composition and Evolution*. Blackwell, Oxford, pp. 27–72.

- Tiepolo, M., Vannucci, R., Oberti, R., Foley, S., Bottazzi, P., Zanetti, A., 2000. Nb and Ta incorporation and fractionation in titanian pargasite and kaersutite: crystal-chemistry constraints and implications for natural systems, *Earth and Planetary Science Letters*, 176 185–201.
- Valizadeh, M.V., Cantagral, J.M., 1975. Premieres donnees radiometriques (K-Ar et Rb-Sr) sur les micas du complexe magmatique du Mont Alvand pres Hamedan (Iran Occidental). *Comptes Rendus Hebdomadares des Seances de l'Academie des Sciences, Serie D, Sciences Naturelles*, 281 1083-1086.
- Vervoot, J.D., Patchett, P.J., Gehrels, G.E., Nutman, A.P. 1996. Constraints on early Earth differentiation from hafnium and neodymium isotopes. *Nature*, 379 624-627.
- White, A.J.R., Allen, C.M., Beams, S.D., Carr, P.F., Champion, D.C., Chappell, B.W., Wyborn, D., Wyborn, L.A.I., 2001. Granite suites and supersuites of eastern Australia. *Australian Journal of Earth Sciences*. 48, 515–530.
- Wilson, M., 1989. *Igneous Petrogenesis: A Global Tectonic Approach*. Chapman and Hall, London, p. 466.
- Wood, D.A., Joron, J.L., Treuil M., Norry M., Tarney, J., 1979. Elemental and Sr isotope variations in basic lavas from Iceland and the surrounding ocean floor. *Contributions to Mineralogy and Petrology*, 70 319-339.
- Yurimoto, H., Duke, E.F., Papike, J.J., Shearer, C.K., 1990. Are discontinuous chondrite-normalized REE patterns in pegmatitic granite systems the results of monazite fractionation. *Geochimica et Cosmochimica Acta*, 54 2141–2145.
- Zen, E-an, 1988, Phase relations of peraluminous granitic rocks and their petrogenetic implications: *Annual Review of Earth and Planetary Sciences*, 16 21–51.